

# A Generic Neighbourhood Filtering Framework for Matrix Fields

Luis Pizarro, Bernhard Burgeth, Stephan Didas, and Joachim Weickert

Mathematical Image Analysis Group,  
Faculty of Mathematics and Computer Science,  
Building E1.1, Saarland University, 66041 Saarbrücken, Germany  
{pizarro,burgeth,didas,weickert}@mia.uni-saarland.de,  
<http://www.mia.uni-saarland.de>

**Abstract.** The *Nonlocal Data and Smoothness* (NDS) filtering framework for greyvalue images has been recently proposed by Mrázek *et al.* This model for image denoising unifies M-smoothing and bilateral filtering, and several well-known nonlinear filters from the literature become particular cases. In this article we extend this model to so-called matrix fields. These data appear, for example, in diffusion tensor magnetic resonance imaging (DT-MRI). Our matrix-valued NDS framework includes earlier filters developed for DT-MRI data, for instance, the *affine-invariant* and the *log-Euclidean* regularisation of matrix fields. Experiments performed with synthetic matrix fields and real DT-MRI data showed excellent performance with respect to restoration quality as well as speed of convergence.

## 1 Introduction

Image denoising and simplification is a ubiquitous task in image processing, and numerous techniques have been developed over the years. These methods are based e.g. on statistical notions, partial differential equations, variational principles and regularisation methods. Nevertheless, a common feature for most of the techniques is an averaging process over the neighbourhood of each pixel. An early example is the *sigma* filter of Lee [1], and the M-smoothers of Chu *et al.* [2] fall also in this category. Polzehl and Spokoiny proposed a technique called *adaptive weights smoothing* [3]. The *W-estimator* by Winkler *et al.* [4] has a close relation to the spatially weighted *M-smoothers* [5]. The *bilateral filter* by Tomasi and Manduchi [6] can be described as a weighted averaging filter as well.

The energy-based approach recently proposed by Mrázek *et al.* [7] combines M-smoothers with bilateral filtering. It is a fairly general nonlocal filtering framework that takes advantage of the so-called *Nonlocal Data and Smoothness* terms, hence referred to as *NDS* in this article. These terms allow for the processing of information from, in principle, arbitrary large neighbourhoods around pixels. The data term rewards similarity of our filtered image to the original one, and hence counteracts the smoothness term which penalises high variations of the evolving image inside a neighbourhood. A thorough investigation of the

NDS-framework and its relation to other filters for grey scale images has been performed in [8] and [9].

The goal of this article is the extension of this rather general filtering framework to matrix-valued data, so-called matrix- or tensor-fields, which we regard as mappings from points of a set in  $\mathbb{R}^d$  into the set  $S(k)$  of real, symmetric  $k \times k$ -matrices. *Diffusion Tensor Magnetic Resonance Imaging* (DT-MRI) is the most prominent source for this data type: This modern medical image acquisition technique associates a real symmetric positive-definite  $3 \times 3$ -matrix to each voxel of the volume under consideration. These matrices, visualised by ellipsoids, indicate the diffusive behaviour of water molecules under thermal Brownian motion, and as such reflect the structure of the surrounding tissue. However, symmetric but possibly indefinite matrix-fields also appear, for example in physics and engineering as general descriptors of anisotropic behaviour. In any case, the data are often corrupted by noise and a filtering and simplification of the matrix fields is necessary. Filtering for processing of positive definite matrix-fields, namely DT-MRI data, based on diffusion and regularisation concepts have been proposed in [10,11], based on differential geometric considerations in [12,13,14,15,16,17,18]. An alternative framework relying on an operator-algebraic view on symmetric matrices provides the ground for filtering and regularisation of matrix fields, positive definite or not, in [19,20].

A short review of the NDS framework in the subsequent Section 2 will reveal that for its applicability the data to be processed have to be elements of a vector space equipped with a metric, and hence be extended to matrix-fields. In Section 3 we show that various filtering approaches described in the recent literature are particular cases of the general matrix-valued NDS framework. We report on experiments in Section 4 pointing out the capabilities and prospects of the NDS methodology. We summarise our contribution in Section 5.

## 2 NDS Framework and Its Extension to Matrix Fields

Let  $f, u \in \mathbb{R}^d$  be discrete  $d$ -dimensional scalar images. In this article we assume  $d = 1, \dots, 3$ , and  $f$  stands for the noisy image while  $u$  represents a processed version of it. Let  $J = \{1, \dots, n\}$  be the index set of all pixels in the images. The pixel position in the  $d$ -dimensional grid is indicated by  $x_i$  ( $i \in J$ ) and  $h_{i,j}^2 = |x_i - x_j|^2$  stands for the square of the Euclidean distance between the two pixel positions  $x_i$  and  $x_j$ . Such quantity will be referred to as *spatial distance*. The *tonal distance* then is the distance between grey values of two pixels, for example  $|u_i - f_j|^2$ . The functional  $E$  of the NDS filter presented in [7] is a linear combination of a data and a smoothness term:

$$\begin{aligned}
 E(u) = & \alpha \sum_{i \in J} \sum_{j \in J} \Psi_D(|u_i - f_j|^2) w_D(|x_i - x_j|^2) \\
 & + (1 - \alpha) \sum_{i \in J} \sum_{j \in J} \Psi_S(|u_i - u_j|^2) w_S(|x_i - x_j|^2). \quad (1)
 \end{aligned}$$

This formulation combines a similarity constraint and a smoothness constraint, which are weighted by a parameter  $\alpha \in [0, 1]$ . The spatial weights  $w_D$  and  $w_S$  take into account the spatial distance between pixel positions  $x_i$  and  $x_j$  in contrast to the tonal weights  $\Psi_D$  and  $\Psi_S$  penalising high deviations between the corresponding grey values. Omitting the details which can be found in [8] the minimiser of this functional is obtained through a fixed-point iteration based on

$$u_i^{k+1} = \frac{\alpha \sum_{j \in J} \Psi'_D \left( |u_i^k - f_j|^2 \right) f_j w_D(h_{i,j}^2) + 2(1 - \alpha) \sum_{j \in J} \Psi'_S \left( |u_i^k - u_j^k|^2 \right) u_j^k w_S(h_{i,j}^2)}{\alpha \sum_{j \in J} \Psi'_D \left( |u_i^k - f_j|^2 \right) w_D(h_{i,j}^2) + 2(1 - \alpha) \sum_{j \in J} \Psi'_S \left( |u_i^k - u_j^k|^2 \right) w_S(h_{i,j}^2)}. \tag{2}$$

Positivity of the denominator is guaranteed if  $\Psi'_{\{S,D\}}(s^2), w_{\{S,D\}}(h^2) > 0$ , i.e., the penalisers are monotonically increasing, hence the right hand side of (2) is a convex combination of grey values  $u_j, f_j$ .

We transfer the scalar fixed point formulation (2) to the matrix-valued setting. We use capital letters  $F_i, U_i$  to denote matrices of a matrix field at position  $x_i$ . An associated fixed point iteration for matrix-fields is given by

$$U_i^{k+1} = H^{-1} \left( \frac{\alpha \sum_{j \in J} \Psi'_D (d(U_i^k, F_j)^2) H(F_j) w_D(h_{i,j}^2) + 2(1 - \alpha) \sum_{j \in J} \Psi'_S (d(U_i^k, U_j^k)^2) H(U_j^k) w_S(h_{i,j}^2)}{\alpha \sum_{j \in J} \Psi'_D (d(U_i^k, F_j)^2) w_D(h_{i,j}^2) + 2(1 - \alpha) \sum_{j \in J} \Psi'_S (d(U_i^k, U_j^k)^2) w_S(h_{i,j}^2)} \right) \tag{3}$$

where we incorporated the following adjustments: The term  $d(A, B)$  denotes a distance measure between the two matrices  $A, B \in S(n)$ . Two instances are of relevance in this article: One is the computationally inexpensive *Frobenius norm* of matrices,

$$d_F(A, B) := \|A - B\|_F \tag{4}$$

with  $\|C\|_F := \sqrt{\text{trace}(C^\top C)}$ . The second one is the *log-Euclidean distance* between matrices in  $S^+(n)$ , i.e., the set of real symmetric positive-semidefinite  $n \times n$ -matrices, [16],

$$d_{LE}(A, B) := \|\ln(A) - \ln(B)\|_F. \tag{5}$$

$H$  in (3) is a function which is applied to a symmetric matrix  $M$ . To this end let  $M$  have the spectral decomposition

$$M = \Lambda \text{diag}(\lambda_1, \dots, \lambda_n) \Lambda^\top$$

where  $\Lambda$  is an orthogonal matrix and  $\text{diag}(\lambda_1, \dots, \lambda_n)$  is a diagonal matrix with the eigenvalues  $\lambda_i$  of  $M$  as non-zero diagonal entries. Then

$$H(M) = \Lambda \text{diag}(H(\lambda_1), \dots, H(\lambda_n)) \Lambda^\top$$

provided  $H$  is defined for each of the scalar values  $\lambda_i$ . In the next section we will see some instances of such mappings that allow us to obtain several filters suggested in the literature as particular cases of our general NDS framework for matrix-fields (3).

### 3 Related Filters within This Framework

The matrix-valued NDS framework offers many degrees of freedom. It can even be considered as an unified approach to M-smoothing ( $\alpha = 1$ ) and bilateral filtering ( $\alpha = 0$ ) for matrix fields. Furthermore, we are able to regain several filtering approaches known from the literature by specifying relevant quantities in (3):

1. *Affine-invariant weighted average* of diffusion tensors [13,14,15,17] with
  - $\alpha = 0$ ,  $\Psi_S(d^2) = d^2$ ,  $w_S = \text{Gaussian}$ ,
  - $\Psi_D$  and  $w_D$  do not play any role,
  - $H(A_j) = A_i^{-\frac{1}{2}} \ln \left( A_i^{-\frac{1}{2}} A_j A_i^{-\frac{1}{2}} \right) A_i^{-\frac{1}{2}}$ .
2. *Log-Euclidean weighted average* of diffusion tensors [16] with
  - the same than in 1, but with  $H(A_j) = \ln(A_j)$ .
3. *Affine-invariant regularisation/interpolation* of tensors fields via a discrete *geodesic marching scheme* [15] with
  - $\lambda = \frac{2 \cdot (1-\alpha)}{\alpha}$ ,  $\Psi_S(d^2) = \text{any}$ ,  $w_S = \text{unit disk}$ ,
  - $\Psi_D(d^2) = d^2$ ,  $w_D = \text{Gaussian}$ ,
  - $H(A_j) = A_i^{-\frac{1}{2}} \ln \left( A_i^{-\frac{1}{2}} A_j A_i^{-\frac{1}{2}} \right) A_i^{-\frac{1}{2}}$ .
4. *Log-Euclidean regularisation/interpolation* of tensors fields via a discrete *geodesic marching scheme* [21] with
  - the same than in 3, but with  $H(A_j) = \ln(A_j)$ .
5. A version of *bilateral filtering* for tensor fields [22] with
  - $\alpha = 0$ ,  $\Psi_S(d^2) = d^2$ ,  $w_S = \mu_1 \cdot d_S + \mu_2 \cdot |x_i - x_j|$  ( $\mu_1, \mu_2 > 0$ ),
  - $\Psi_D$  and  $w_D$  do not play any role,
  - $H(A_j) = \ln(A_j)$ .

Note that most of the mentioned methods do not exploit the utilisation of nonlocal information in the data/similarity term, i.e.,  $\alpha = 0$ , or the radius of action of their smoothness term is restricted to the unit circle. In this sense, we can consider generalised versions of those methods within the scope of the neighbourhood filtering framework for matrix fields proposed in Section 2. Of course, further specialised filters for tensor fields can be generated for specific applications by appropriately setting the matrix-valued NDS model.

In Section 4 we will demonstrate the denoising capabilities of our general framework regarding two prominent special cases. Their performance will be evaluated with respect to restoration quality and speed of convergence on synthetically generated tensor fields and on real DT-MRI data.

### 4 Comparative Results

In this section, we test our general filtering framework for matrix fields (3) on synthetic and real-world data. Fig. 1 shows a 2-D dataset consisting of  $32 \times 32$  matrices. The data are represented as ellipsoids via the level sets of the quadratic

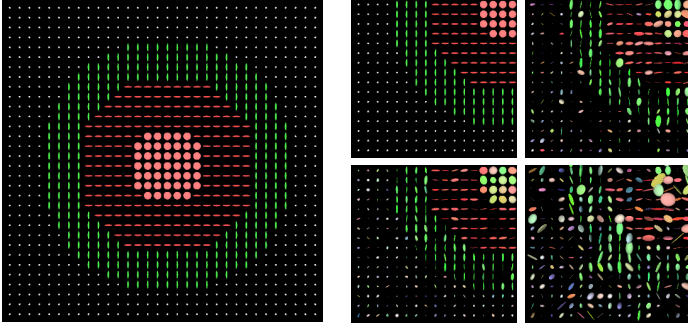


**Fig. 1.** Synthetic data. **Left:** Original matrix field with homogeneous structures consisting of four types of matrices. **Middle Top:** Scaled-up region of the original matrix field. **Middle Bottom:** Version degraded with  $\sigma = 500$ . **Right Top:** Version degraded with  $\sigma = 1000$ . **Right Bottom:** Version degraded with  $\sigma = 2000$ .

form  $x^\top A^{-2}x = const.$ ,  $x \in \mathbb{R}^3$ , associated with a matrix  $A \in S^+(3)$ . By using  $A^{-2}$  the lengths of the semi-axes of the ellipsoid correspond directly with the three eigenvalues of the matrix  $A$ . To demonstrate the denoising capabilities, we additively degrade our uncorrupted synthetic matrix field  $(U_i)_{i \in J}$  with  $U_i \in S^+(3)$ , with random positive definite matrices  $(N_i)_{i \in J}$ , i.e.,  $F_i = |U_i + N_i|$ , where  $F_i$  is the corrupted version of  $U_i$ . The eigenvalues of the noise matrix  $N_i$  stem from a Gaussian distribution with vanishing mean and standard deviation  $\sigma$ . The eigenvectors of the noise matrix result in choosing three uniformly distributed angles and rotating  $N_i$  by these angles around the coordinate axes. Finally, we take the absolute value for positive definiteness. Considering that the eigenvalues of the original matrix field are in the range  $[1000, 4000]$ , the noisy tensor fields for  $\sigma = 500, 1000, 2000$  are shown in Fig. 1.

#### 4.1 Two Prominent Filtering Models: NDS-I and NDS-LE

We focus on two models: The NDS-I model when choosing  $H(U) = U$ , and the NDS-LE (*log-Euclidean*) model for  $H(U) = \ln(U)$ . Independently of the model, the choice of the tonal penalisers  $\Psi_D$  and  $\Psi_S$  is done following two strategies:

- (P.1) Penalisers requiring no parameters at all. We use the Whittaker-Tikhonov penaliser for the data term, i.e.,  $\Psi_D(d^2) = d^2$ , and the Nashed-Scherzer penaliser [23] for the smoothness term, i.e.,  $\Psi_S(d^2) = \beta d^2 + \sqrt{d^2 + \epsilon^2}$ , with  $\epsilon = 1$  and  $\beta = \frac{1}{10\epsilon}$ .
- (P.2) Penalisers with better edge-preservation properties, paying the price of including a parameter  $\lambda$  as a *contrast parameter*. We use the classic Perona-Malik penaliser, [24],  $\Psi(d^2) = \lambda^2 \ln\left(1 + \frac{d^2}{\lambda^2}\right)$  in both the data and the smoothness term. In this case the parameter  $\lambda$  is estimated as the 1%-quantile of the distribution of distances for a particular distance measure  $d$  and noise level  $\sigma$ .

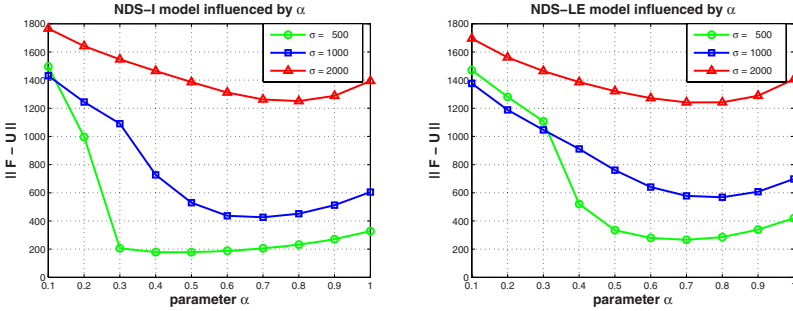


**Fig. 2.** Influence of the parameter  $\alpha$  on the NDS-I model (*left*) and the NDS-LE model (*right*) under different levels of noise  $\sigma = 500, 1000, 2000$ . The penalisers (P.2) are used in both models. NDS-I uses  $d_F$  as tensor distance, while NDS-LE uses  $d_{LE}$ . The size parameters of the spatial weight functions were set to  $r_D = r_S = 1$ .

Also independent of the filtering model, we consider two tensor distance measures: the Frobenius distance  $d_F$  (4) and the log-Euclidean distance  $d_{LE}$  (5). Last but not least, we use a soft window  $w_r(h^2) = \exp\left(-\frac{h^2}{2r^2}\right)$  as spatial weight function for both the data and the smoothness term, with size parameters  $r_D$  and  $r_S$ , respectively.

### 4.2 Influence of Parameters

Although we have specified the NDS-I and the NDS-LE models in the previous section, note that there are still some free parameters that will directly influence the denoising capabilities of our filters. Namely, the parameter  $\alpha$  that counterbalances the contributions of the data and the smoothness term in (3), and the size parameters  $r_D$  and  $r_S$  of the spatial weight functions that allow smoothing within large neighbourhoods. Fig. 2 shows the influence of the parameter  $\alpha$  on the NDS-I and NDS-LE models with respect to the *reconstruction quality* measured as the norm of the difference between the original matrix field  $F$  and the denoised field  $U$ , i.e.,  $\|F - U\| := \left(\sum_{i=1}^N \|F_i - U_i\|_F\right)^{1/2}$ . The non-trivial steady-state is shown for  $\alpha \in (0, 1]$ . We see that there is a value  $\hat{\alpha}$  for which the restoration quality is optimal.

We now want to quantify the influence of the size parameters  $r_D, r_S$ . Increasing the parameters naturally increases the number of arithmetic operations in (3). However, the restoration quality might be improved and the steady-state can be reached in a shorter time. If we vary the parameters in the range  $[0, 4]$  there are 25 possible combinations  $(r_D, r_S)$  that we arrange as  $O_0, \dots, O_{24}$  following the ordering shown in Fig. 3 (*top*). The diagonal lines in the figure group the combinations according to *complexity order* (CO), i.e., configurations with equal/increasing number of operations. Fig. 3 (*bottom*) shows the restoration quality (*left*), the logarithmic computational time (*middle*), and the overall performance (*right*) of the NDS-I model. The last measurement is simply the

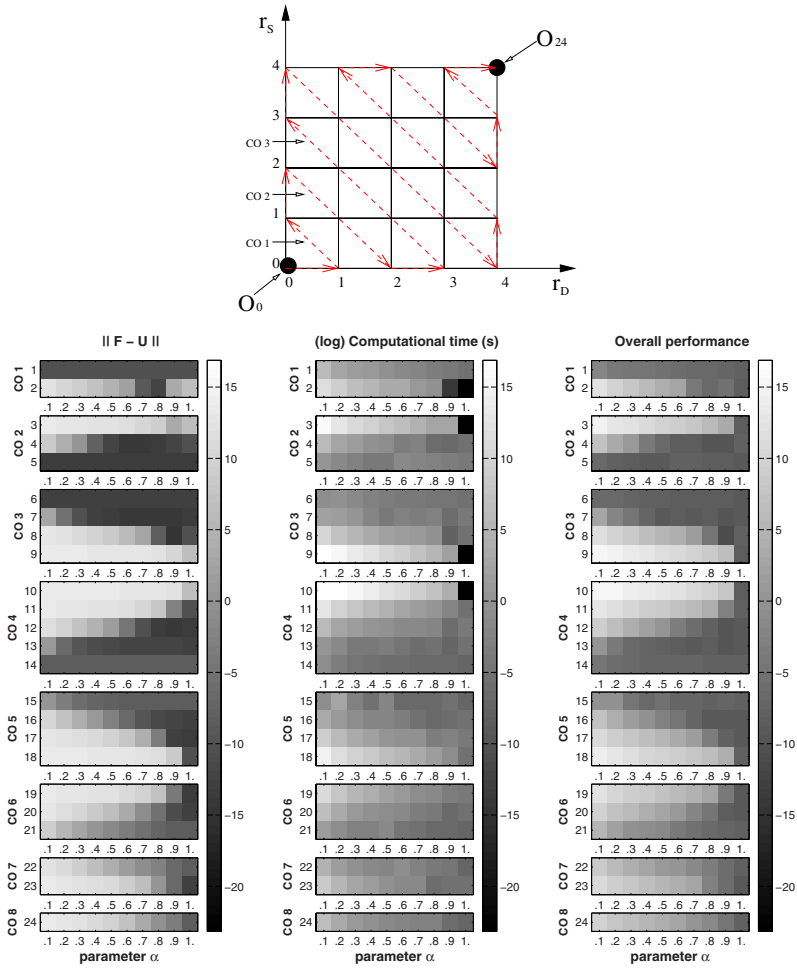


**Fig. 3. Top:** Ordering  $O_0, \dots, O_{24}$  for the different combinations of  $(r_D, r_S)$  grouped according to complexity order  $CO_i$  ( $i = 1, \dots, 8$ ). **Bottom, left to right:** Normalised restoration quality, computational time, and overall performance of the NDS-I model in filtering the noisy tensor field with noise level  $\sigma = 1000$ . The penalisers (P.2) are used with distance measure  $d_F$ .

mean between the first two normalised measurements. We see that the configuration with the best performance in terms of quality and fast convergence is  $O_8 = (r_D, r_S) = (1, 2)$  for  $\alpha = 0.9$ . It is worth mentioning that the configurations  $O_5 = (2, 0)$ ,  $O_6 = (3, 0)$  and  $O_{14} = (4, 0)$ , lead to good results despite the fact that they allow only for the incorporation of neighbourhood information in the data term. This is in agreement with the findings in [9]. The authors argued that filters based only on nonlocal M-smoothers can produce similar results to those obtained via classical variational/regularisation methods. The observations presented here are also valid for the NDS-LE filtering model.

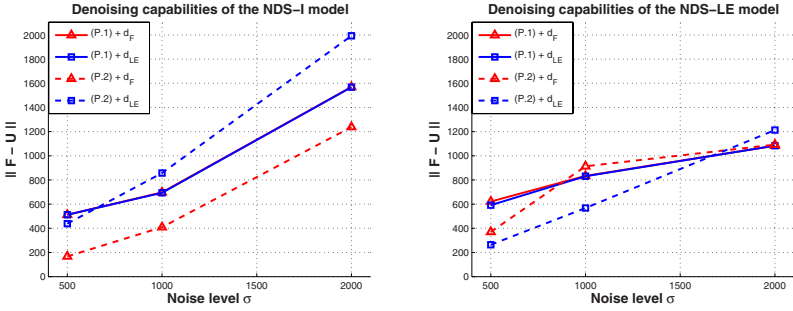


**Fig. 4. Left:** Restoration quality achieved by the NDS-I model using independently both type of penalisers (P.1) and (P.2), as well as both distance measures  $d_F$  and  $d_{LE}$ . **Right:** The same for the NDS-LE model. All parameters  $r_D$ ,  $r_S$  and  $\alpha$  were optimised.

**Table 1.** Best filtering results for both the NDS-I and the NDS-LE models under noise level  $\sigma = 500, 1000, 2000$ . All parameters were optimised.

$\sigma$	Model	$r_D$	$r_S$	$\alpha$	$\ F - U\ $	Iter.	Time (s)
500	NDS-I	2	3	0.9	167	33	0.69
	NDS-LE	1	2	0.9	264	71	19.31
1000	NDS-I	1	2	0.9	409	72	0.71
	NDS-LE	2	0	0.2	568	236	57.97
2000	NDS-I	2	0	0.1	1238	256	1.91
	NDS-LE	2	1	0.9	1214	32	9.50

### 4.3 Comparing the Models

In this section we juxtapose the NDS-I and the NDS-LE models. We evaluate their performance in filtering the noisy tensor fields shown in Fig. 1 for different levels of noise  $\sigma = 500, 1000, 2000$ .

Fig. 4 depicts the restoration quality achieved by both the NDS-I and the NDS-LE frameworks. We notice that both models achieve the best performance when the Perona-Malik penalisers (P.2) are employed. With respect to the tensor distance measures, it turned out that the NDS-I model works better with the Frobenius distance, while the NDS-LE model in principle performs better with the log-Euclidean distance<sup>1</sup>. The best results are outlined in Table 1. It is clear that both models benefit from nonlocal smoothing by considering  $r_D, r_S > 0$ . Note that the NDS-I model is considerably faster than the NDS-LE variant, the latter being burdened with the additional computation of logarithms and exponentials of matrices. Computations have been performed on a 1.86 GHz Intel Core 2 Duo processor (without exploiting multitasking) executing C code.

<sup>1</sup> It is slightly worse for the noise level  $\sigma = 2000$ .

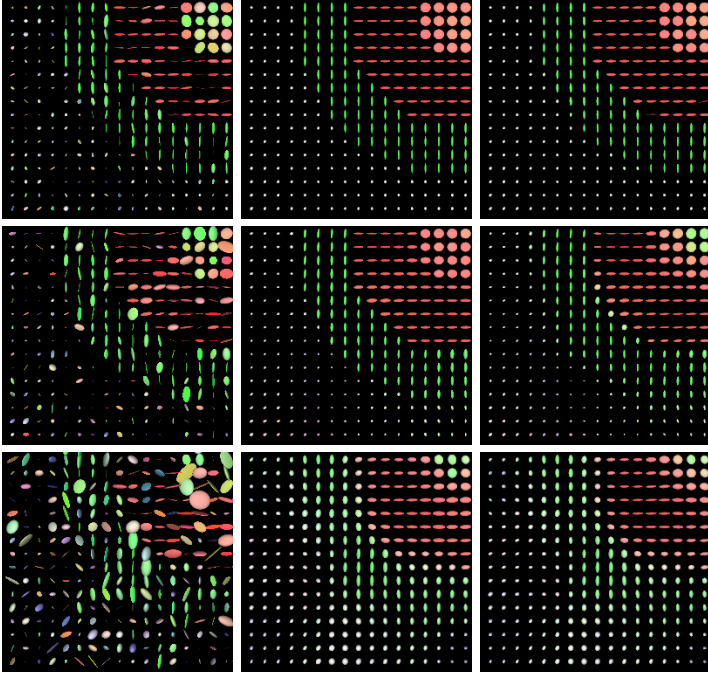


**Fig. 5. Left Column, Top to Bottom:** Matrix-fields degraded with noise level  $\sigma = 500, 1000, 2000$ . **Middle Column, Top to Bottom:** Steady-state results of Table 1 for NDS-I filtering of noisy tensor fields with noise level  $\sigma = 500, 1000, 2000$ . **Right Column, Top to Bottom:** The same for NDS-LE filtering.

Fig. 5 shows the denoised matrix fields for the results presented in Table 1. At any noise level NDS-I filtering produces a slightly more homogeneous output, in accordance with the original, than the NDS-LE model. This effect is most prominent in the case of the filtering of the noisy field with noise level  $\sigma = 1000$ , but it is also present in the filtered version of the noisy field associated with  $\sigma = 500$ , in particular in the lower part of the inner ring. Particularly noticeable in the example for  $\sigma = 1000$  is that both the edges of the image structures and the anisotropy of the matrices are better preserved if filtered with the NDS-I model than with the NDS-LE variant. Moreover, the eigenvalue-swelling-effect on the edges is more perceptible in the NDS-LE model than in the NDS-I model.

#### 4.4 Test on DT-MRI Data

In DT-MRI, noisy *diffusion weighted images* (DWIs) are used to estimate the diffusion tensors via regression analysis. It is known that DWIs are perturbed by Rician noise [25]. However, the noise distribution of the diffusion tensors obeys a multivariate Gaussian distribution, as it has been statistically proven by Pajevic and Bassler [26]. Here, as it was done in the previous section, we directly apply our filtering framework to the tensor field, and not to the scalar DWIs. We use a

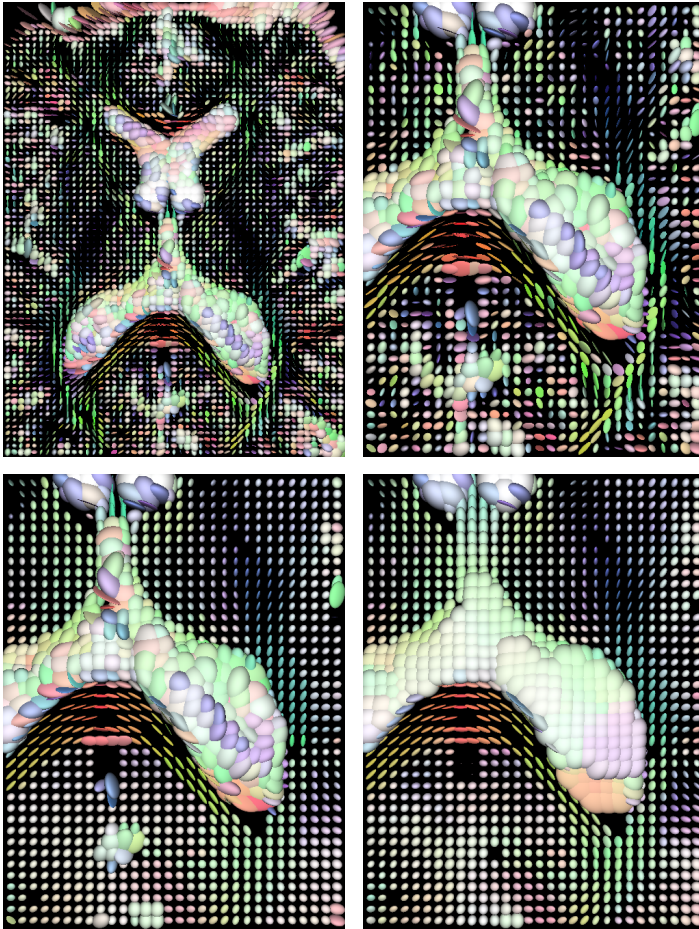


**Fig. 6.** Denoising capabilities of the NDS-I model on real-world data. **Top Left:** 2-D section ( $50 \times 70 \times 1$  voxels) of a 3-D DT-MRI dataset showing the corpus callosum. **Top Right:** Scaled-up region of the corpus callosum. **Bottom Left:** Filtered region using the NDS-I model with penalisers (P.2) and distance measure  $d_F$ , and parameters  $\lambda = 140$  (0.01%-quantile),  $r_D = 1$ ,  $r_S = 2$ , and  $\alpha = 0.9$ . 386 iterations ( $\approx 4$  seconds) were needed to reach the steady-state. **Bottom Right:** The same with parameters  $\lambda = 355$  (1%-quantile). 184 iterations ( $\approx 2$  seconds) needed.

real-world 3-D DT-MRI dataset of a human head consisting of a  $128 \times 128 \times 30$ -field of positive definite matrices. Fig. 6 shows a 2-D section of the corpus callosum, which has been filtered using the NDS-I model. We see that after denoising edges are well preserved and localised, and zones with different anisotropy are clearly distinguished. These characteristics are important in applications such as tractography [27] and the study of diseases associated with certain abnormalities in the brain anatomy [28].

## 5 Conclusions

In its fixed point form the NDS filtering framework model has been extended in full generality to the matrix-valued setting. It generalises several known filtering concepts suggested in the literature for the filtering of DT-MRI data including those employing the log-Euclidean framework to preserve positive definiteness of the data. Despite its many degrees of freedom it does not require sophisticated tuning to outperform previous related filtering concepts concerning computational time and denoising quality. We emphasise that our methodology is generic and thus not restricted to DT-MRI denoising. It can be applied to any multi-valued image with values in the space of symmetric matrices. In a future work we will make full use of the directional and shape information of the local structures to steer the filtering process.

**Acknowledgements.** We gratefully acknowledge partial funding by the *Deutscher Akademischer Austauschdienst* (DAAD), grant A/05/21715.

## References

1. Lee, J.S.: Digital image smoothing and the sigma filter. *Computer Vision, Graphics, and Image Processing* 24, 255–269 (1983)
2. Chu, C.K., Glad, I.K., Godtlielsen, F., Marron, J.S.: Edge-preserving smoothers for image processing. *Journal of the American Statistical Association* 93, 526–541 (1998)
3. Polzehl, J., Spokoiny, V.: Adaptive weights smoothing with applications to image restoration. *Journal of the Royal Statistical Society, Series B* 62, 335–354 (2000)
4. Winkler, G., Aurich, V., Hahn, K., Martin, A.: Noise reduction in images: Some recent edge-preserving methods. *Pattern Recognition and Image Analysis* 9, 749–766 (1999)
5. Griffin, L.D.: Mean, median and mode filtering of images. *Proceedings of the Royal Society of London A* 456, 2995–3004 (2000)
6. Tomasi, C., Manduchi, R.: Bilateral filtering for gray and colour images. In: *Proc. of the 1998 IEEE International Conference on Computer Vision, Bombay, India*, pp. 839–846. Narosa Publishing House (1998)
7. Mrázek, P., Weickert, J., Bruhn, A.: On robust estimation and smoothing with spatial and tonal kernels. In: Klette, R., Kozera, R., Noakes, L., Weickert, J. (eds.) *Geometric Properties for Incomplete Data*, pp. 335–352. Springer, Heidelberg (2006)
8. Didas, S., Mrázek, P., Weickert, J.: Energy-based image simplification with non-local data and smoothness terms. In: Iske, A., Levesley, J. (eds.) *Algorithms for Approximation*, pp. 51–60. Springer, Heidelberg (2006)
9. Pizarro, L., Didas, S., Bauer, F., Weickert, J.: Evaluating a general class of filters for image denoising. In: Ersbøll, B.K., Pedersen, K.S. (eds.) *SCIA 2007. LNCS*, vol. 4522, pp. 601–610. Springer, Heidelberg (2007)
10. Tschumperlé, D., Deriche, R.: Diffusion tensor regularization with constraints preservation. In: *Proc. of the 2001 IEEE Computer Society Conference on Computer Vision and Pattern Recognition (CVPR 2001)*, vol. 1, pp. 948–953 (2001)
11. Weickert, J., Brox, T.: Diffusion and regularization of vector- and matrix-valued images. In: Nashed, M.Z., Scherzer, O. (eds.) *Inverse Problems, Image Analysis, and Medical Imaging. Contemporary Mathematics*, vol. 313, AMS, Providence (2002)

12. Chéfd'hotel, C., Tschumperlé, D., Deriche, R., Faugeras, O.: Regularizing flows for constrained matrix-valued images. *Journal of Mathematical Imaging and Vision* 20, 147–162 (2004)
13. Batchelor, P.G., Moakher, M., Atkinson, D., Calamante, F., Connolly, A.: A rigorous framework for diffusion tensor calculus. *Magnetic Resonance in Medicine* 53, 221–225 (2005)
14. Moakher, M.: A differential geometry approach to the geometric mean of symmetric positive-definite matrices. *SIAM Journal on Matrix Analysis and Applications*, 735–747 (2005)
15. Pennec, X., Fillard, P., Ayache, N.: A Riemannian framework for tensor computing. *International Journal of Computer Vision* 66, 41–66 (2006)
16. Arsigny, V., Fillard, P., Pennec, X., Ayache, N.: Log-Euclidean metrics for fast and simple calculus on diffusion tensors. *Magnetic Resonance in Medicine* 56, 411–421 (2006)
17. Fletcher, P.T., Joshi, S.: Riemannian geometry for the statistical analysis of diffusion tensor data. *Signal Processing* 87, 250–262 (2007)
18. Gur, Y., Sochen, N.: Coordinate-free diffusion over compact Lie-groups. In: Sgalari, F., Murli, A., Paragios, N. (eds.) *SSVM 2007*. LNCS, vol. 4485, pp. 580–591. Springer, Heidelberg (2007)
19. Burgeth, B., Didas, S., Florack, L., Weickert, J.: A generic approach to diffusion filtering of matrix-fields. *Computing* 81, 179–197 (2007)
20. Steidl, G., Setzer, S., Popilka, B., Burgeth, B.: Restoration of matrix fields by second order cone programming. *Computing* 81, 161–178 (2007)
21. Fillard, P., Arsigny, V., Pennec, X., Ayache, N.: Joint estimation and smoothing of clinical DT-MRI with a log-Euclidean metric. Research Report RR-5607, INRIA, Sophia-Antipolis, France (2005)
22. Hamarneh, G., Hradsky, J.: Bilateral filtering of diffusion tensor magnetic resonance images. *IEEE Transactions on Image Processing* 16, 2463–2475 (2007)
23. Nashed, M.Z., Scherzer, O.: Least squares and bounded variation regularization with nondifferentiable functionals. *Numerical Functional Analysis and Optimization* 19, 873–901 (1998)
24. Perona, P., Malik, J.: Scale space and edge detection using anisotropic diffusion. *IEEE Transactions on Pattern Analysis and Machine Intelligence* 12, 629–639 (1990)
25. Gudbjartsson, H., Patz, S.: The Rician distribution of noisy MRI data. *Magnetic Resonance in Medicine* 34, 910–914 (1995) [published erratum appears in *Magnetic Resonance in Medicine* 36, 332 (1996)]
26. Pajevic, S., Basser, P.J.: Parametric and non-parametric statistical analysis of DT-MRI data. *Journal of Magnetic Resonance* 161, 1–14 (2003)
27. Mori, S., van Zijl, P.C.: Fiber tracking: principles and strategies - a technical review. *NRM in Biomedicine* 15, 468–480 (2002)
28. Nucifora, P.G., Verma, R., Lee, S.K., Melhem, E.R.: Diffusion-tensor MR imaging and tractography: Exploring brain microstructure and connectivity. *Radiology* 245, 367–384 (2007)